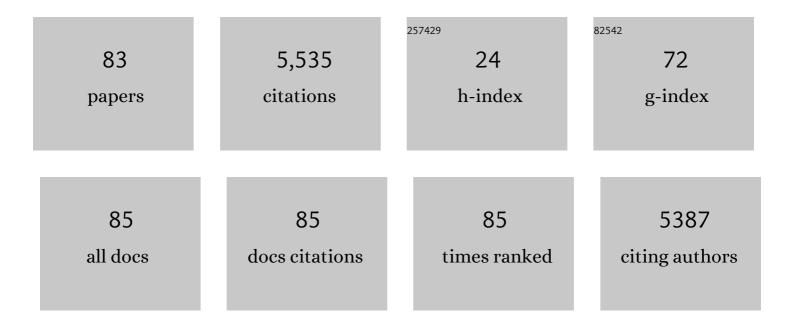
Hermann Scharfetter

List of Publications by Year in descending order

Source: https://exaly.com/author-pdf/8394418/publications.pdf Version: 2024-02-01



#	Article	IF	CITATIONS
1	Joint multiâ€field T <scp>₁</scp> quantification for fast field ycling MRI. Magnetic Resonance in Medicine, 2021, 86, 2049-2063.	3.0	4
2	Spin–spin relaxation of nuclear quadrupole resonance coherences and the important role of degenerate energy levels. Molecular Physics, 2020, 118, e1743888.	1.7	4
3	Aspects of structural order in 209Bi-containing particles for potential MRI contrast agents based on quadrupole enhanced relaxation. Molecular Physics, 2019, 117, 935-943.	1.7	2
4	1H relaxation and dynamics of triphenylbismuth in deuterated solvents. Molecular Physics, 2019, 117, 921-926.	1.7	0
5	Multi-quantum quadrupole relaxation enhancement effects in ²⁰⁹ Bi compounds. Journal of Chemical Physics, 2019, 150, 184309.	3.0	8
6	Estimation of the magnitude of quadrupole relaxation enhancement in the context of magnetic resonance imaging contrast. Journal of Chemical Physics, 2019, 150, 184306.	3.0	11
7	Tris(2-Methoxyphenyl)Bismuthine Polymorphism Characterized by Nuclear Quadrupole Resonance Spectroscopy. Crystals, 2019, 9, 446.	2.2	0
8	Highâ€Field Detection of Biomarkers with Fast Field ycling MRI: The Example of Zinc Sensing. Chemistry - A European Journal, 2019, 25, 8236-8239.	3.3	7
9	Comparison of fast field-cycling magnetic resonance imaging methods and future perspectives. Molecular Physics, 2019, 117, 832-848.	1.7	15
10	Quadrupole relaxation enhancement and polarisation transfer in DMSO solution of [Bi(NO ₃) ₃ (H ₂ O) ₃]*18-crown-6 in solid state. Molecular Physics, 2019, 117, 944-951.	1.7	1
11	¹ H spin–lattice relaxation in water solution of ²⁰⁹ Bi counterparts of Gd ³⁺ contrast agents. Molecular Physics, 2019, 117, 927-934.	1.7	3
12	Predicting quadrupole relaxation enhancement peaks in proton <i>R</i> ₁ -NMRD profiles in solid Bi-aryl compounds from NQR parameters. Molecular Physics, 2019, 117, 910-920.	1.7	3
13	A cryostatic, fast scanning, wideband NQR spectrometer for the VHF range. Journal of Magnetic Resonance, 2018, 286, 148-157.	2.1	8
14	R 1 dispersion contrast at high field with fast field-cycling MRI. Journal of Magnetic Resonance, 2018, 290, 68-75.	2.1	14
15	Model – free approach to quadrupole spin relaxation in solid ²⁰⁹ Bi-aryl compounds. Physical Chemistry Chemical Physics, 2018, 20, 23414-23423.	2.8	6
16	Tuning Nuclear Quadrupole Resonance: A Novel Approach for the Design of Frequency-Selective MRI Contrast Agents. Physical Review X, 2018, 8, .	8.9	8
17	²⁰⁹ Bi quadrupole relaxation enhancement in solids as a step towards new contrast mechanisms in magnetic resonance imaging. Physical Chemistry Chemical Physics, 2018, 20, 12710-12718.	2.8	25
18	Assessment of skin permeability to topically applied drugs by skin impedance and admittance. Physiological Measurement, 2017, 38, N138-N150.	2.1	7

#	Article	IF	CITATIONS
19	An electronically tuned wideband probehead for NQR spectroscopy in the VHF range. Journal of Magnetic Resonance, 2016, 271, 90-98.	2.1	10
20	A no-tune no-match wideband probe for nuclear quadrupole resonance spectroscopy in the VHF range. Measurement Science and Technology, 2014, 25, 125501.	2.6	4
21	The Agile Library for Biomedical Image Reconstruction Using GPU Acceleration. Computing in Science and Engineering, 2013, 15, 34-44.	1.2	15
22	A deterministic approach to the adapted optode placement for illumination of highly scattering tissue. Biomedical Optics Express, 2012, 3, 1732.	2.9	6
23	High-performance image reconstruction in fluorescence tomography on desktop computers and graphics hardware. Biomedical Optics Express, 2011, 2, 3207.	2.9	9
24	Phase synchronization of hemodynamic variables and respiration during mental challenge. International Journal of Psychophysiology, 2011, 79, 401-409.	1.0	50
25	Using the topological derivative for initializing a Markov-chain Monte Carlo reconstruction in fluorescence tomography. Proceedings of SPIE, 2011, , .	0.8	1
26	Uncertainty analysis for fluorescence tomography with Monte Carlo method. , 2011, , .		0
27	Enhancing Impedance Imaging Through Multimodal Tomography. IEEE Transactions on Biomedical Engineering, 2011, 58, 3215-3224.	4.2	14
28	Imaging artifacts in magnetic induction tomography caused by the structural incorrectness of the sensor model. Measurement Science and Technology, 2011, 22, 015502.	2.6	18
29	Nonlinear Inversion Schemes for Fluorescence Optical Tomography. IEEE Transactions on Biomedical Engineering, 2010, 57, 2723-2729.	4.2	14
30	Anisotropic conductivity tensor imaging using magnetic induction tomography. Physiological Measurement, 2010, 31, S135-S145.	2.1	11
31	A marker belt design to eliminate the motion artifacts in magnetic induction tomography. , 2010, , .		0
32	Adaptation and focusing of optode configurations for fluorescence optical tomography by experimental design methods. Journal of Biomedical Optics, 2010, 15, 016024.	2.6	6
33	Total variation regularization for nonlinear fluorescence tomography with an augmented Lagrangian splitting approach. Applied Optics, 2010, 49, 3741.	2.1	36
34	Effects of Stimuli on Cardiovascular Reactivity Occurring at Regular Intervals During Mental Stress. Journal of Psychophysiology, 2010, 24, 48-60.	0.7	21
35	Magnetic induction pneumography: a planar coil system for continuous monitoring of lung function via contactless measurements. Journal of Electrical Bioimpedance, 2010, 1, 56-62.	0.9	5

Resolution and stability analysis of 16 channel magnetic induction tomography. , 2009, , .

0

#	Article	IF	CITATIONS
37	The effect of receiver coil orientations on the imaging performance of magnetic induction tomography. Measurement Science and Technology, 2009, 20, 105505.	2.6	20
38	Reconstruction artefacts in magnetic induction tomography due to patient's movement during data acquisition. Physiological Measurement, 2009, 30, S165-S174.	2.1	23
39	Optimum Receiver Array Design for Magnetic Induction Tomography. IEEE Transactions on Biomedical Engineering, 2009, 56, 1435-1441.	4.2	24
40	Feasibility of head imaging using multi-frequency magnetic induction tomography. , 2009, , .		0
41	Sensor optimization for fluorescence optical tomography by experimental design methods. , 2009, , .		3
42	13th International Conference on Electrical Bioimpedance and 8th Conference on Electrical Impedance Tomography (Graz, Austria, 29 August–2 September 2007). Physiological Measurement, 2008, 29, E1-2.	2.1	3
43	Indicator for hydration balance during haemodialysis based on anisotropic FEM. Physiological Measurement, 2008, 29, S479-S489.	2.1	1
44	Magnetic induction tomography: comparison of the image quality using different types of receivers. Physiological Measurement, 2008, 29, S417-S429.	2.1	13
45	Hardware for quasi-single-shot multifrequency magnetic induction tomography (MIT): the Graz Mk2 system. Physiological Measurement, 2008, 29, S431-S443.	2.1	36
46	Magnetic induction tomography: evaluation of the point spread function and analysis of resolution and image distortion. Physiological Measurement, 2007, 28, S313-S324.	2.1	15
47	Imaging of local lung ventilation under different gravitational conditions with electrical impedance tomography. Acta Astronautica, 2007, 60, 281-284.	3.2	5
48	Spectroscopic 16 channel magnetic induction tomograph: The new Graz MIT system. , 2007, , 452-455.		14
49	Magnetic Induction Tomography: A feasibility study of brain oedema detection using a finite element human head model. IFMBE Proceedings, 2007, , 480-483.	0.3	16
50	Determination of local phase changes in lung ventilation by EIT during continuous postural changes. IFMBE Proceedings, 2007, , 528-530.	0.3	0
51	Correction of systematic errors in frequency differential magnetic induction tomography. IFMBE Proceedings, 2007, , 476-479.	0.3	Ο
52	Magnetic InductionTomography: The influence of the coil configuration on the spatial resolution. , 2007, , 456-459.		1
53	Single-Step 3-D Image Reconstruction in Magnetic Induction Tomography: Theoretical Limits of Spatial Resolution and Contrast to Noise Ratio. Annals of Biomedical Engineering, 2006, 34, 1786-1798.	2.5	36
54	Solution of the inverse problem of magnetic induction tomography (MIT) with multiple objects: analysis of detectability and statistical properties with respect to the reconstructed conducting region. Physiological Measurement, 2006, 27, S249-S259.	2.1	7

#	Article	IF	CITATIONS
55	A multifrequency magnetic induction tomography system using planar gradiometers: data collection and calibration. Physiological Measurement, 2006, 27, S271-S280.	2.1	46
56	Reconstruction of the shape of conductivity spectra using differential multi-frequency magnetic induction tomography. Physiological Measurement, 2006, 27, S237-S248.	2.1	34
57	Direct reconstruction of tissue parameters from differential multifrequency EITin vivo. Physiological Measurement, 2006, 27, S93-S101.	2.1	14
58	Fat and Hydration Monitoring by Abdominal Bioimpedance Analysis: Data Interpretation by Hierarchical Electrical Modeling. IEEE Transactions on Biomedical Engineering, 2005, 52, 975-982.	4.2	25
59	A new type of gradiometer for the receiving circuit of magnetic induction tomography (MIT). Physiological Measurement, 2005, 26, S307-S318.	2.1	53
60	Monitoring of lung edema using focused impedance spectroscopy: a feasibility study. Physiological Measurement, 2005, 26, 185-192.	2.1	25
61	Solution of the inverse problem of magnetic induction tomography (MIT). Physiological Measurement, 2005, 26, S241-S250.	2.1	79
62	Detection of brain oedema using magnetic induction tomography: a feasibility study of the likely sensitivity and detectability. Physiological Measurement, 2004, 25, 347-354.	2.1	92
63	Measurement of liver iron overload by magnetic induction using a planar gradiometer: preliminary human results. Physiological Measurement, 2004, 25, 315-323.	2.1	32
64	Planar gradiometer for magnetic induction tomography (MIT): theoretical and experimental sensitivity maps for a low-contrast phantom. Physiological Measurement, 2004, 25, 325-333.	2.1	24
65	Bioelectrical impedance analysis?part I: review of principles and methods. Clinical Nutrition, 2004, 23, 1226-1243.	5.0	2,089
66	Bioelectrical impedance analysis—part II: utilization in clinical practice. Clinical Nutrition, 2004, 23, 1430-1453.	5.0	1,643
67	Numerical Simulation of the Eddy Current Problem in Magnetic Induction Tomography for Biomedical Applications by Edge Elements. IEEE Transactions on Magnetics, 2004, 40, 623-626.	2.1	33
68	Fast calculation of the sensitivity matrix in magnetic induction tomography by tetrahedral edge finite elements and the reciprocity theorem. Physiological Measurement, 2004, 25, 159-168.	2.1	50
69	Sodium intake does not influence bioimpedance-derived extracellular volume loss in head-down rest. Aviation, Space, and Environmental Medicine, 2004, 75, 1036-41.	0.5	4
70	Biological tissue characterization by magnetic induction spectroscopy (MIS): requirements and limitations. IEEE Transactions on Biomedical Engineering, 2003, 50, 870-880.	4.2	113
71	Numerical solution of the general 3D eddy current problem for magnetic induction tomography (spectroscopy). Physiological Measurement, 2003, 24, 545-554.	2.1	64
72	Direct estimation of Cole parameters in multifrequency EIT using a regularized GaussÂNewton method. Physiological Measurement, 2003, 24, 437-448.	2.1	23

#	Article	IF	CITATIONS
73	Sensitivity maps for low-contrast perturbations within conducting background in magnetic induction tomography. Physiological Measurement, 2002, 23, 195-202.	2.1	47
74	Magnetic induction tomography: hardware for multi-frequency measurements in biological tissues. Physiological Measurement, 2001, 22, 131-146.	2.1	118
75	Sensitivity maps and system requirements for magnetic induction tomography using a planar gradiometer. Physiological Measurement, 2001, 22, 121-130.	2.1	72
76	Multi frequency electrical impedance tomography. COMPEL - the International Journal for Computation and Mathematics in Electrical and Electronic Engineering, 2001, 20, 828-847.	0.9	3
77	Assessing abdominal fatness with local bioimpedance analysis: basics and experimental findings. International Journal of Obesity, 2001, 25, 502-511.	3.4	70
78	Ein Ansatz zur Optimierung der ProzeßSteuerung bei der Hänodialyse. Automatisierungstechnik, 1999, 47, 38-48.	0.8	0
79	Inductively Coupled Wideband Transceiver for Bioimpedance Spectroscopy (IBIS)a. Annals of the New York Academy of Sciences, 1999, 873, 322-334.	3.8	18
80	Exchange of Alkali Trace Elements in Hemodialysis Patients:A Comparison with Na ⁺ and K ⁺ . Nephron, 1999, 83, 226-236.	1.8	13
81	A model of artefacts produced by stray capacitance during whole body or segmental bioimpedance spectroscopy. Physiological Measurement, 1998, 19, 247-261.	2.1	79
82	Effect of postural changes on the reliability of volume estimations from bioimpedance spectroscopy data. Kidney International, 1997, 51, 1078-1087.	5.2	76
83	Influence of ionic shifts during dialysis on volume estimations with multifrequency impedance analysis. Medical and Biological Engineering and Computing, 1997, 35, 96-102.	2.8	32